

Hydrogen Gas Sensors Utilizing Perylene-Imide Derivatives with Pyridyl Rings

K. Sato, K. Hino, H. Takahashi* and J. Mizuguchi
Department of Applied Physics, Graduate School of Engineering,
Yokohama National University, Yokohama, Japan
* Toyo Ink Engineering Co. Ltd., Tokyo, Japan

Abstract

Perylene-imide derivatives are industrially important pigments that exhibit a variety of shades from red *via* maroon to black. In the present investigation, we have synthesized novel perylene-imide derivatives with pyridyl rings in an attempt to apply them for H₂ gas sensors based on proton acceptors. The two N atoms of the pyridyl rings which work as proton acceptors are found to remain unbounded in the solid state according to X-ray analysis and are thus available for protonation necessary for H₂ gas sensors. The H₂ gas sensors exhibit a significant change in electrical resistivity by about three orders of magnitude even under 0.05 % H₂.

Keywords: perylene-imide, hydrogen gas sensor, crystal structure

1 Introduction

Perylene-imide derivatives are well known organic pigments that exhibit a variety of shades in the solid state from red *via* maroon to black [1]. These materials have attracted attention as photoconductors for photoreceptors as well as materials for optical disks [2].

We have carried out a series of investigations on H₂ gas sensors utilizing a high proton affinity of organic pigments that have pyridyl rings connected directly to the chromophore [3]. 1,4-Diketo-3,6-bis-(4'-pyridyl)-pyrrolo-[3,4-*c*]pyrrole (DPPP), for example, is a dipyridyl derivative that possesses a high proton affinity because of the N atoms of the pyridyl rings. A drastic change in shade as well as electrical conductivities by several orders of magnitude was observed due to protonation at the N atom. Therefore, DPPP had newly attracted attention as a material for H₂ gas sensor.

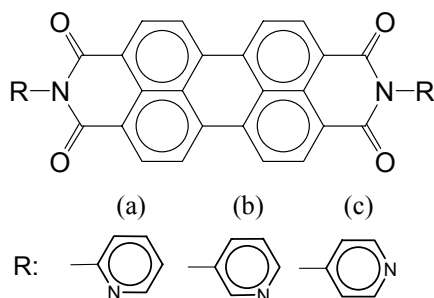


Figure 1: Molecular conformation (a) OPP, (b) MPP and (c) PPP.

In the present investigation, we have synthesized novel perylene-imide derivatives with pyridyl rings in

an attempt to apply them for H₂ gas sensors. There are *ortho*, *meta* and *para*-pyridyl derivatives abbreviated to OPP, MPP and PPP, respectively (Fig. 1). These compounds are found to exhibit resistivity changes of about three orders of magnitude, even for 0.05 % H₂, but their sensitivity is slightly different, depending on the site of the N atom. The present paper deals with the characteristics of H₂ gas sensors based upon OPP, MPP and PPP. Details on the structure analysis are also presented in Appendix.

2 Experiment

2.1 Structure of the H₂ sensor

Fig. 2(a) shows the interdigital electrodes made of ITO (Indium-Tin-Oxide). The sensor based on the interdigital electrodes includes two important functions: one is to dissociate H₂ into protons and the other is to detect the change in electrical conductivity due to protonation. In order to dissociate H₂, we incorporate a thin layer of Pd since H₂ is known to be unstable on Pd. At the same time, we apply a rather high electric field between electrodes in order to assist the dissociation of H₂. The successful result is obtained by sputtering Pd directly on the interdigital electrodes in the form of islands as shown in Fig. 2(b), followed by application of the perylene-imide derivatives by vacuum evaporation. The sensor structure is ITO/Pd/Perylene/ITO.

H₂ gas is first adsorbed on the surface of sensor material and encounters Pd to dissociate into protons as shown in Fig. 2(b). At this moment, protonation takes place at the N atom of the pyridyl ring to release one electron. This contributes to the decrease in resistivity.

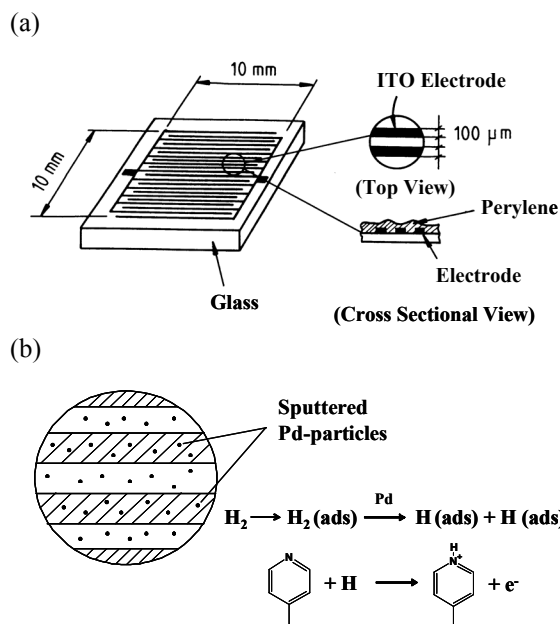


Figure 2: (a) Interdigital electrodes and (b) magnified Pd-sputtered electrodes.

2.2 Synthesis and crystal growth

OPP was synthesized by heating perylene-3,4,9,10-tetracarboxylic dianhydride and 2-aminopyridine at 490 K in dimethylnaphtalene for 3 hours. Likewise, MPP and PPP were synthesized with 3-aminopyridine and 4-aminopyridine, respectively. The products were then purified three times by sublimation at 760 K, using a two-zone furnace. Single crystals of OPP and MPP were grown from the vapor phase. On the other hand, single crystals of PPP were grown by recrystallization from solution in 1-chloronaphtalene using an autoclave.

3 Results and Discussion

3.1 Performance of the H₂ gas sensor

Figure 3(a) shows the change in resistivity of the MPP sensor as a function of bias voltage when the sensor is exposed to 100 % H₂. The resistivity decreases drastically by four orders of magnitude at room temperature. Likewise, the OPP and PPP sensors show similar sensitivity as shown in Figs. 3(b) and 3(c), respectively. All three sensors exhibit a high sensitivity, but their sensitivity is slightly different, depending on the site of the N atom. The present remarkable resistivity change is obviously attributed to the fact that the N atom of the pyridyl ring remains unbounded in the solid state as shown by structure analysis given in Appendix, without being utilized for the formation of, for example, intermolecular hydrogen bonds.

The resistivities of the MPP sensor for the H₂ concentrations of 0.05, 0.1, 1 and 10 % are shown in Fig. 4. It should be noted that the resistivity

diminishes by three orders of magnitude even for the H₂ concentration of 0.05 %. Furthermore, the resistivity is found to decrease linearly with increasing H₂ concentration, because Fig. 4 is a log-log plot of the resistivity.

Figure 5 shows the buildup of the MPP sensor signals as a function of time. The buildup time (80 % of the maximum time) is 1 s where the gain is *ca.* 3 × 10⁴. This indicates that the response is quite rapid in the gain range of several factors. The signal builds up and down and then remains nearly constant. When H₂ is switched off, the signal decays and comes back to the initial state in 4 seconds.

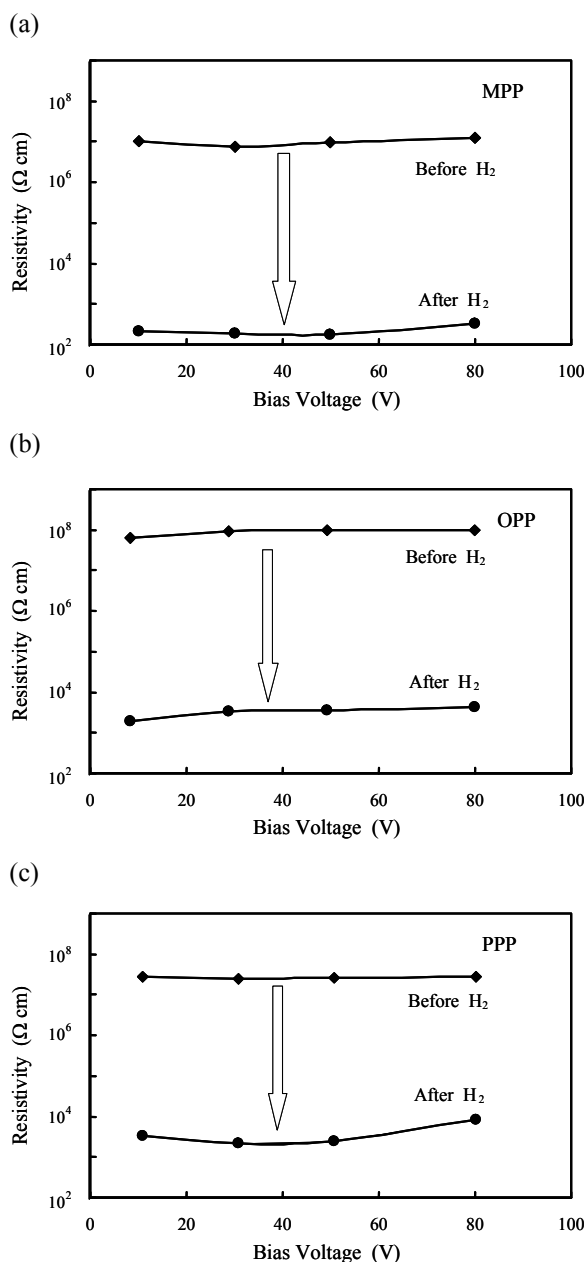


Figure 3: Changes in resistivity of the sensors before and after H₂ (100 %) as a function of applied voltage. (a) MPP, (b) OPP and (c) PPP.

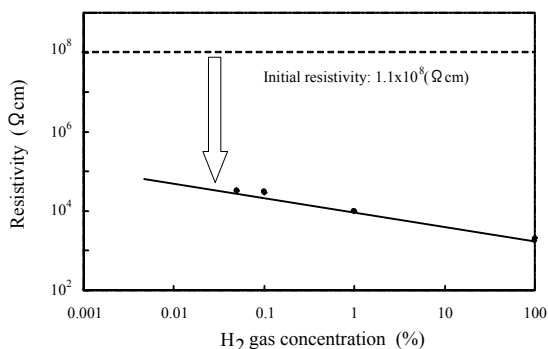


Figure 4: Log-log plot of the resistivity of the MPP sensor and H₂ concentration: 0.05, 0.1, 1 and 100 % H₂.

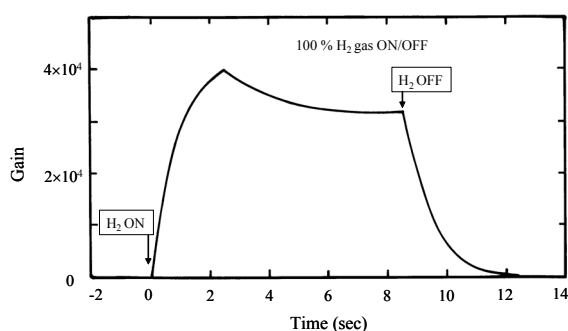


Figure 5: Build up and build down of the MPP sensor signal as a function of time.

3.2 Determination of the charge carrier

Figure 6 shows the experimental setup for the determination of charge carriers on the basis of the Seebeck effect. A soldering iron was used as the heating element as well as the counter electrode to measure thermoelectromotive force that appears due to a temperature between two electrodes through the perylene-imide derivatives.

An *n*-type Si chip was used as the reference. If the potential at the soldering rod appears positive, the charge carrier is then determined to be electrons. On the contrary, the charge carrier is holes if the potential is negative.

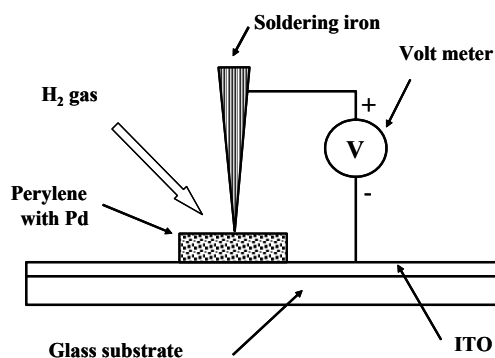


Figure 6: Experimental setup for measurements of Seebeck coefficient.

A positive potential of 0.8 mV appeared when the MPP sensor was exposed to H₂. Likewise, the OPP and PPP sensors exhibited positive potential. This clearly indicates that the current is due to electrons in the present sensor. This bears out our proposed operation principle shown in Fig. 2.

3.3 Influence of various gases on the gas sensor

We have studied the influence of various gases on the sensing characteristic: CH₄ (1 %), CO (2 %), CO₂ (24 %), NO (0.6 %) and SO₂ (0.2 %) and H₂O moisture. The sensor was exposed to these gases with a flow rate of 2 l/min. No noticeable effect (*i.e.* less than 0.1 % in resistivity change) was recognized for these gases, indicating that the sensors are free from the influence of ambient gases.

4 Conclusions

High-performance H₂ gas sensors have been developed that utilize a proton affinity of perylene-imide derivatives with pyridyl rings. The two pyridyl rings are found to remain free (*i.e.* unbounded) as shown by X-ray analysis and are available for protonation necessary for H₂ gas sensors. Reductions of resistivity by about three orders of magnitude are achieved at room temperature for 0.05 % H₂.

Furthermore, the process is reversible and the build up and build down times of the sensors are quite rapid. No noticeable effect of ambient gases (CH₄, CO, CO₂, NO and SO₂ gases together with H₂O moisture) is found in the present sensors.

References

- [1] Herbst, W. and Hunger, K., *Industrial Organic Pigments*, 2nd Edition, VCH, Weinheim, pp 467-475 (1993).
- [2] Mizuguchi, J., "Electronic characterization of *N,N'*-bis(2-phenylethyl)perylene-3,4:9,10-bis(dicarboximide) and its application to optical disks", *J. Appl. Phys.*, **84**, 4479-4486 (1998).
- [3] Takahashi, H. and Mizuguchi, J., "Hydrogen Gas Sensor Utilizing a High Proton Affinity of Pyrrolopyrrole Derivatives", *J. Electrochem. Soc.*, **152**, H69-H73 (2005).
- [4] Mizuguchi, J., Hino, K., Sato, K., Takahashi, H. and Suzuki, S., "*N,N'*-Di-2-pyridylperylene-3,4:9,10-bis(dicarboximide)", *Acta Cryst.*, **E61**, o437-o439 (2005).
- [5] Mizuguchi, J., Hino, K., Sato, K., Takahashi, H. and Suzuki, S., "*N,N'*-Di-3-pyridylperylene-3,4:9,10-bis(dicarboximide)", *Acta Cryst.*, **E61**, o434-o436 (2005).
- [6] Hino, K., Sato, K., Takahashi, H., Suzuki, S. and Mizuguchi, J., "*N,N'*-Di-4-pyridylperylene-3,4:9,10-bis(dicarboximide)", *Acta Cryst.*, **E61**, o440-o441 (2005).

Appendix

Table 1 details the crystallographic parameters for OPP [4], MPP [5] and PPP [6].

The two independent molecules, *A* and *B*, of OPP are characterized by the same molecular C_i symmetry. The molecular conformations of these molecules are quite similar, but twist angle of the pyridyl rings is different. The angles between each of the pyridyl rings and the perylene-imide skeleton are 77.7° in molecule *A* and 72.8° in molecule *B*. Molecules *A* and *B* are stacked alternately along the *b* axis, as shown Fig. 7(a).

The molecule of MPP is characterized by C_i symmetry. The pyridyl rings twisted by 54.9° in the same direction. The molecules are stacked in a 'hunter's fence' fashion (*viz.* when viewed from the side, molecules, slipped by 45° within molecular stacks, cross each other in a fence-like structure) along the *b* axis, as shown in Fig. 7(b).

On the other hand, the molecule of PPP is characterized by C_2 symmetry. The pyridyl rings are twisted by 74.5° in the opposite direction. The molecules are stacked along the *c* axis with a tilt angle of 31.5° between adjacent molecules as shown in Fig. 7(c).

It is to be noted that two N atoms in each pyridyl rings of OPP, MPP and PPP remain free (*i.e.* unbounded), indicating to be able to accept protons. For this reason, all three derivatives are ideal for applications of H_2 gas sensors.

Table 1: Crystallographic parameters

	OPP (<i>ortho</i>)	MPP (<i>meta</i>)	PPP (<i>para</i>)
Formula	$C_{34}H_{16}N_4O_4$	$C_{34}H_{16}N_4O_4$	$C_{34}H_{16}N_4O_4$
Crystal system	monoclinic	monoclinic	orthorhombic
Space group	$P2_1/c$	$P2_1/n$	$Pccn$
Molecular symmetry	C_i	C_i	C_2
<i>Z</i>	4	2	4
<i>a</i> , Å	17.599(1)	15.422(2)	21.232(2)
<i>b</i> , Å	7.1705(5)	3.8275(6)	15.890(2)
<i>c</i> , Å	20.679(2)	19.282(3)	6.9311(8)
α , °	-	-	-
β , °	111.004(5)	103.29(1)	-
γ , °	-	-	-
Density ($g\ cm^{-3}$)	1.49	1.63	1.55
R_1	0.062	0.039	0.074

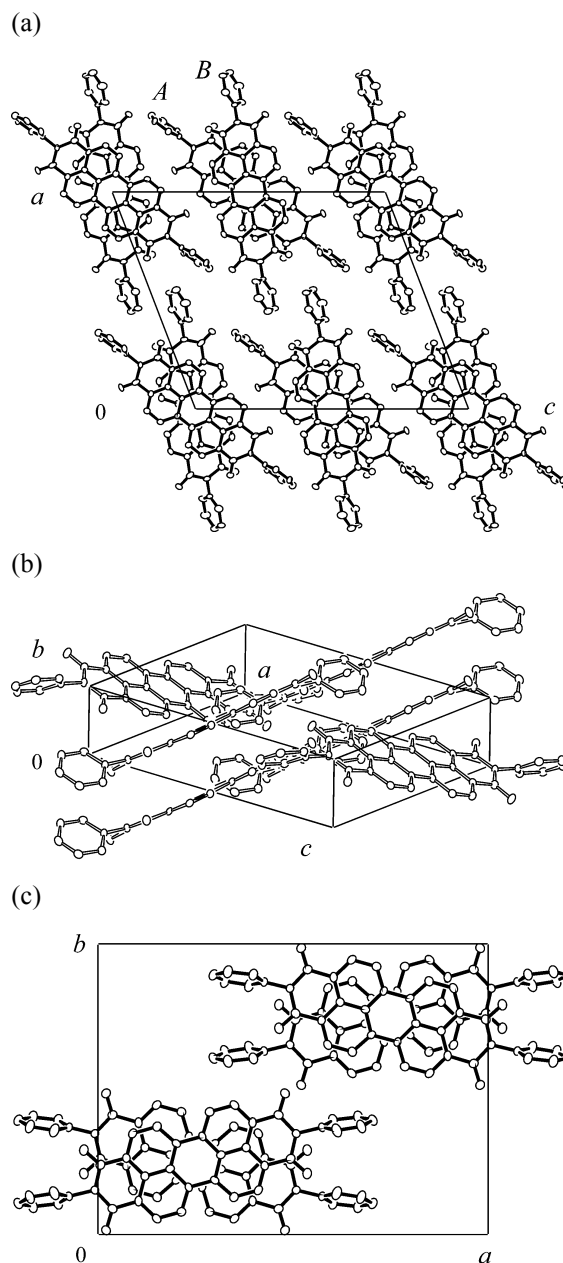


Figure 7: Molecular arrangement (a) projection of OPP on to the *ac* plane, (b) the packing arrangement of MPP and (c) projection of PPP on to the *ab* plane.